AIAA JOURNAL
Vol. 39, No. 6, June 2001

Inferring Propeller Inflow and Radiation from Near-Field Response, Part 1: Analytic Development

R. J. Minniti* and W. K. Blake†
U.S. Naval Surface Warfare Center, West Bethesda, Maryland 20817-5700
and
T. J. Mueller‡
University of Notre Dame, Notre Dame, Indiana 46556

In general, the physics of the relationship between the pressure field surrounding a rotating propeller in subsonic flow and the flow characteristics is understood. However, quantification of this relationship in a way that allows engineering analysis of propeller noise is limited by complete definition of the inflow distortions. Therefore, a way of inferring this relationship and the distortion characteristics unobtrusively and in situ has been developed. The technique is based on the assumption that measurements of the unsteady pressure on the blades are available. From the pressures, the technique predicts the radiated acoustic far field, infers incoming flow characteristics, and defines Green's function between the near and far pressure fields. The analysis combines theoretical and empirical treatments of pressure data to infer the acoustic quantities. Thus, the turbulence ingestion problem is approached in a practical manner without the need for many of the simplifying assumptions required by purely theoretical means. The technique is developed for use on experimental data. The technique is subsequently applied to a propeller operating downstream of large-scale, mean-flow distortions, and ingesting broadband turbulence (Minniti, R. J., Blake, W. K., and Mueller, T. J., "Inferring Propeller Inflow and Radiation from Near-Field Response, Part 2: Empirical Application," *AIAA Journal*, Vol. 39, No. 6, 2001, pp. 1037–1046).

Nomenclature

B	=	blade number
c	=	airfoil chord
c_0	=	speed of sound
G_{PT}	=	Green's function between acoustic pressure and unsteady thrust
H_{lp}	=	transfer function between unsteady lift and unsteady pressure
$\boldsymbol{k}$	=	turbulence wave vector
k_0	=	acoustic wave number, ω/c_0
L	=	unsteady lift
L_3	=	blade span
P	=	far-field acoustic pressure
p	=	unsteady pressure on airfoil surface
R_{ij}	=	cross correlation between unsteady pressure on blades i and j
$\boldsymbol{r}$	=	acoustic field observation position vector
Se	=	Sears function
S_{2D}	=	aerodynamic admittance function incorporating spanwise variation of flow
T	=	unsteady propeller thrust
t	=	time
U	=	mean velocity
u	=	unsteady velocity
$\boldsymbol{x}$	=	blade position vector
β	=	blade summation gain
γ_{ij}	=	coherence between unsteady pressure on blades i and j
$\bar{\gamma}$	=	average blade pitch
η	=	direction cosine
θ	=	angle of acoustic observation
Λ_3	=	spanwise integral length scale of turbulence
ξ	=	flag denoting even or odd blade number
ρ	=	density
Φ_x	=	autospectrum of quantity x
Φ_{xy}	=	cross spectrum between quantities x and y
φ	=	phase of acoustic field
Ω	=	propeller shaft rate
ω	=	circular frequency

Subscripts

l	=	quantities associated with section lift
Σ	=	quantities associated with sum of ring array
1	=	chordwise, scalar component of a vector
2	=	transverse, scalar component of a vector
3	=	spanwise, scalar component of a vector

Superscripts

0	=	$n=0$ summation associated with axial force component
1	=	$n=1$ summation associated with transverse force component

Introduction: Problem Statement

PROPELLERS and axial flow fans usually operate downstream of atmospheric disturbances or flow obstructions that produce large-scale and small-scale turbulence. Even if turbulent flow is not present in the stationary reference frame, spatially nonuniform mean flows translate to periodic gusts in the rotating reference frame of the propeller and cause unsteady pressure on the blade surfaces. This unsteady pressure produces unsteady force that, when summed over the entire propeller, contributes to unsteady thrust. Unsteady thrust radiates noise in the fashion of a dipole and, as such, dominates the far-field acoustic spectrum at low frequency. The physics of the relationship between the acoustic source strength of the propeller/turbulence interaction, the turbulence intensity and the turbulence correlation length, is generally understood. However, quantification of this relationship in a way that allows engineering analysis of propeller noise is limited by the capability of empirical or analytical methods to define the inflow distortions. Thus, a method for inferring these distortions and their relation to noise production unobtrusively and in situ with fewer simplifying assumptions is of interest.

Received 20 July 1999; revision received 20 November 2000; accepted for publication 4 December 2000.

*Mechanical Engineer, Signatures Directorate, Carderock Division.
†Chief Research Scientist, Signatures Directorate, Carderock Division.
‡Roth-Gibson Professor, Department of Aerospace and Mechanical Engineering. Associate Fellow AIAA.

Previous research has advanced the understanding of the relations among inflow conditions, unsteady thrust, and noise generation. Sevik[1] was one of the early pioneers to investigate the unsteady force on propellers in turbulent flow. His model sought to predict thrust spectra for propellers with an isotropic turbulent approach flow. However, he assumed that the turbulent length scales were small and each eddy interacted with only one blade. As such, the resulting thrust spectrum contained only the broadband components of the propeller response and did not show peaks or haystacks near the harmonics of the blade passage frequency. Blake[2] extended this model to include blade-to-blade correlation of lift due to turbulent length scales larger than the blade spacing and predicted haystacks in the continuum around the blade rate harmonics. However, the results of the two models were not married into a single analytical form. When the work of Sevik[1] and Blake[2] was used as a base point, Martinez[3–5] advanced the theory by correctly estimating blade-to-blade correlation in the theoretical model. He posed that the propeller rotation effectively decreased the blade spacing relative to the length scale of the turbulence. Therefore, even for length scales smaller than the blade spacing, the predicted blade-to-blade correlation of unsteady loading caused both broadband and narrowband components of the propeller response to appear in the predicted thrust spectrum.

By necessity, even in this improved model, the turbulent flow was considered to be either isotropic or to have uniform spatial decay of correlation. In real flows, isotropic turbulence does not exist or only approximately exists for small ranges of conditions. Additionally, the small-scale turbulence is often superimposed on larger scale distortions and has nonuniform spatial correlation due to the presence of upstream bodies. These types of flows are difficult to describe by point-to-point measurements of the flow. Therefore, as quantification of the real flows becomes harder, an empirical method to infer the information from the acoustic response is convenient for eliminating acoustic sources in propellers. Of particular interest is a method of interpreting information about the global nature of the flow from the acoustic signature and unsteady pressure measured at the blade surfaces.

This interpretation fits into the general category of an inverse solution. The traditional order of direct solution is to start with the assumption that the inflow conditions are known, solve for the pressure near field, and extend the results to the acoustic far field. In contrast, the inverse solution determines blade surface pressure from the acoustic far field and then projects the results to infer inflow characteristics. Inverse methods have received little attention in the acoustic community. However, Grace et al.[6,7] have established the theoretical basis for the inverse solution of a single airfoil. Their solution is based on the assumption that the airfoil is infinitely thin. Thus, the governing equations of the pressure field are simplified to a single relation. This relation is inverted numerically to give the near-field pressures on the airfoil surface from the far-field pressures. Then, by the use of the unsteady airfoil theory of Sears,[8] the incoming flow is inferred from the near-field pressure. Since this initial work, Patrick-Grace and Atassi[9] have advanced the work to include finite span effects.

The current analysis combines direct and inverse methods to exploit the propellers' own geometry as an in situ transducer for sampling the flow. The inverse methods are similar to those discussed earlier, except that the methods have been extended to the more complicated case of the multiblade propeller ingesting unsteady flow composed of both small-scale turbulence and large-scale, mean-flow distortions. The direct methods have been seeded with empirical data to reduce the number of assumptions about propeller response or inflow characteristics. Comparison of the results of the theoretical and empirically seeded methods yields a greater understanding of the propeller response. Finally, the method is derived with the intended application to a propeller in subsonic flow ($M_\infty < 0.15$). As such, the analysis will likely become inaccurate in transonic and supersonic flow.

Analytical Development of Propeller Response

The analysis of the propeller response is complex, and it is helpful to give a graphical road map of the techniques. The flowchart in Fig. 1 is an outline for the analysis characterizing propeller response in this paper. In Fig. 1, direct solutions run from the left and inverse solutions from the right. At each step in the process, arrows indicate the flow of information and summarize the major points of the analysis. Many of the equations and relations used in the statement of the analysis are rigorously developed elsewhere. Because this is inappropriate for the scope of this paper, the relations have been modified and applied toward the objective of completing the analysis with an appropriate reference stated.

Point Pressure Response

Many researchers have studied the response of an isolated airfoil to an incoming gust. However, the general method proposed by Sears[8] is the most relevant in the present context due to ease of application to unsteady velocity and pressure data. Specifically, the method relates unsteady pressure and lift to unsteady velocity using a generic pressure distribution and a flow-dependent aerodynamic admittance function. Sears considered the flow about a flat plate at zero angle of attack encountering a sinusoidal upwash. When the linearized Euler equations subject to boundary conditions at the body surface and in the wake are used, the chordwise distribution of a single-frequency component of the unsteady pressure jump was given to be

$$\Delta p(x_1, \omega) = 2\rho u_2(\omega) U \sqrt{\frac{c/2 - x_1}{c/2 + x_1}} Se\left(\frac{\omega c}{2U}\right) \tag{1}$$

where $Se(\omega c/2U)$ is the Sears function. The quantity $\omega c/2U$ is often referred to as the reduced frequency k_1^* and can be thought of as the ratio between the airfoil half-chord and the convective wavelength of the gust based on Taylor's hypothesis. The chordwise distribution given by the radical on the right-hand side of Eq. (1) is that of classical steady thin airfoil theory, which the Sears solution must approach in the limit of zero reduced frequency. Note that this definition is off from a more traditional statement of the Sears solution by a minus sign.

When the more complex case of turbulence interaction with an airfoil section is addressed, the unsteady pressure difference between the upper and lower surfaces of an airfoil has been given by a number of investigators in the form

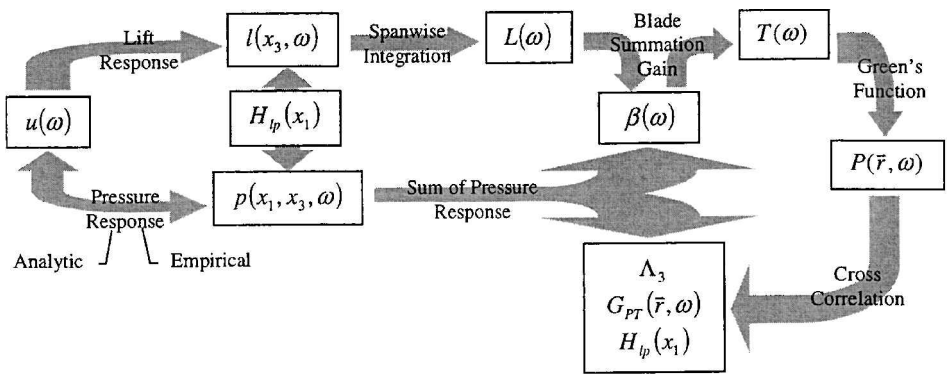

Fig. 1 Flowchart of propeller response analysis.

$$\Delta p(x_1, x_3, k_1, k_3, \omega, t) = 2\rho U u_2(k_1, k_3, \omega) \times \sqrt{\frac{c/2 - x_1}{c/2 + x_1}} S_{2D}\left(\tfrac{1}{2}k_1 c, \tfrac{1}{2}k_3 c\right) \exp[i(k_3 x_3 - \omega t)] \quad (2)$$

which is Eq. (11–36) from Blake.[2] The function $S_{2D}(\frac{1}{2}k_1 c, \frac{1}{2}k_3 c)$ is an aerodynamic admittance that reflects not only the classical chordwise behavior of unsteady lift of the Sears admittance[8] but also addresses variation of the incoming flow along the spanwise direction. Filotas,[10,11] Amiet,[12] Reissner,[13] and Graham[14] are among the investigators who have given analytic or numerical statements of this function. However, if flow lines of constant phase run along the span, that is, $k_3 = 0$, and Taylor's hypothesis of frozen convection holds, that is, $k_1 \approx \omega/U$, the form of Eq. (1) is recovered, and the two admittance functions are equivalent in the limiting case.

Blade Lift Response

The integration of the pressure jump along the chord gives the section lift. Sears[8] found an analytical solution for a single-frequency component of the section lift by integrating the distribution of Eq. (1) to be

$$\frac{dL(\omega)}{dx_3} = \pi\rho c U u_2(\omega) Se\left(\frac{\omega c}{2U}\right) \quad (3)$$

Equation (3) will hold for large-scale distortions with little radial variation of the unsteady flow, as is the case with spanwise-coherent, mean-flow distortions ingested by a propeller with unskewed blades. For these inflow types, accurate description of the total blade response can be estimated by spanwise, strip-theory integration of Eq. (3). However, for the general case of turbulence ingestion, radial variation of the unsteady flow with finite correlation exists. This variation will produce spanwise-coherent lift over regions of limited extent, greatly complicating the integration.

Therefore, a more complete definition of the blade response based on Eq. (2) is required. After integration of Eq. (2) over the chord, a single-frequency component of the blade response to all of the turbulent wave vector components is

$$L(\omega) = \pi\rho c U \int_{-L_3/2}^{L_3/2}\int_{-\infty}^{\infty}\int_{-\infty}^{\infty} u_2(k_1, k_3, \omega) \times S_{2D}\left(\frac{1}{2}k_1 c, \frac{1}{2}k_3 c\right) e^{ik_3 x_3}\, dk_1\, dk_3\, dx_3$$
$$= \pi\rho c U L_3 \int_{-\infty}^{\infty}\int_{-\infty}^{\infty} u_2(k_1, k_3, \omega) S_{2D} \times \left(\frac{1}{2}k_1 c, \frac{1}{2}k_3 c\right)\left(\frac{\sin\frac{1}{2}k_3 L_3}{\frac{1}{2}k_3 L_3}\right) dk_1\, dk_3 \quad (4)$$

where the variations of c, U, and S_{2D} with radial location are assumed negligible relative to changes in unsteady velocity (or at least uncorrelated with them). Accordingly, the blade lift spectrum is

$$\Phi_L(\omega) = \pi^2\rho^2(cL_3)^2 U^2 \int_{-\infty}^{\infty}\int_{-\infty}^{\infty} \Phi_u(k_1, k_3, \omega) \times \left|S_{2D}\left(\frac{1}{2}k_1 c, \frac{1}{2}k_3 c\right)\right|^2 \left(\frac{\sin\frac{1}{2}k_3 L_3}{\frac{1}{2}k_3 L_3}\right)^2 dk_1\, dk_3 \quad (5)$$

At this point, a separable model for the turbulence is introduced with the accompanying assumption of frozen convection (see Blake[2] pp. 735–752 for the complete development of the unsteady blade lift due to turbulent flow ingestion). It is further assumed that the span is substantially larger than the radial macroscale, Λ_3, of the turbulence. Thus, the blade lift becomes

$$\Phi_L(\omega) = \pi^2\rho^2(cL_3)^2 U^2 \frac{\Lambda_3}{\pi}\Phi_u(\omega)\left|Se\left(\frac{\omega c}{2U}\right)\right|^2 \times \int_{-\infty}^{\infty}\left(\frac{\sin\frac{1}{2}k_3 L_3}{\frac{1}{2}k_3 L_3}\right)^2 dk_3 \quad (6)$$

The sine integral has an exact value of $2\pi/L_3$, which yields

$$\Phi_L(\omega) = \pi^2\rho^2(cL_3)^2 U^2\left[|Se(\omega c/2U)|^2(2\Lambda_3/L_3)\right]\Phi_u(\omega) \approx \pi^2\rho^2(cL_3)^2 U^2\left|S_{2D}\left(\tfrac{1}{2}k_1 c, \tfrac{1}{2}k_3 c\right)\right|^2\Phi_u(\omega) \quad (7)$$

The second approximated equality is given to show the use of the multiplicative factor Λ_3 to account for the uncorrelated spanwise stations of lift along the propeller blade. Thus, the preceding result in the first equality reverts to use of the Sears strip aerodynamics[8] as opposed to any analytical treatment of the effect of spanwise wave number on the aerodynamic response.

When the similarities between Eqs. (1–3) and (7) are noted, a transfer function between the section lift and the pressure can be stated for both the specific and general case as

$$\frac{\Phi_l(\omega)}{\Phi_{\Delta p}(x_1, \omega)} = |H_{lp}(x_1)|^2 = \frac{\pi^2 c^2}{4}\left(\frac{c/2 + x_1}{c/2 - x_1}\right) \quad (8)$$

where it has been assumed that no relative phase exists between the pressure jump and lift. As defined, the transfer function incorporates only the chordwise integration of the pressure to find lift and not the aerodynamic admittance. This definition is frequency and velocity independent, which makes it a generic transfer function. When function is applied to Eq. (7), the blade lift spectrum is given in terms of the pressure jump spectrum as

$$\Phi_L(\omega) = 2\Lambda_3 L_3 |H_{lp}(x_1)|^2 \Phi_{\Delta p}(x_1, \omega) \quad (9)$$

In this statement of blade response, if Eq. (2) is used to estimate the unsteady pressure, contributions of turbulence away from the planform of the blade are neglected. Thus, the blades are assumed to interact with the turbulent eddies individually, as described by Sevik.[1] However, an empirical measurement of the pressure does not suffer this shortcoming. Therefore, the measured unsteady pressure can be used to quantify empirically blade-to-blade coupling of lift and characterize total propeller response.

As stated after Eq. (4), variation in c, U, and Sears number Se were considered secondary effects in the development of Eq. (9). However, the statement can now be used in a crude sense in strip theory integration where these variations are considered and the span L_3 is replaced by the incremental span Δx_3:

$$\frac{\Delta\Phi_L(x_3, \omega)}{\Delta x_3} = 2\Lambda_3 |H_{lp}(x_1, x_3)|^2 \Phi_{\Delta p}(x_1, x_3, \omega) \quad (10)$$

Thus, Eq. (10) has generalized Eq. (3) to hold at every spanwise station, and the unsteady lift is related to the unsteady pressure jump without the use of a frequency-dependent admittance function. Because no general analytic treatment of the admittance function accounting for the finite thickness, camber, and angle of attack of a cascade airfoil exists, the measurement of unsteady pressure is the most direct way to measure unsteady loading.

Unsteady Thrust and Acoustic Prediction Using a Blade Summation Gain

Analysis of the propeller thrust response is often built from an analytical model that addresses local coupling of lift on blades in a cascade. It is then assumed that the cascade response characterizes the propeller response, as shown in Fig. 2. The blade-to-blade interactions are important to interpreting the unsteady response of the propeller; however, the effect of the original circumferentially

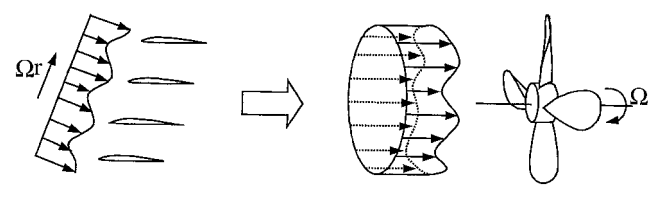

Fig. 2 Assembly of propeller response from airfoil cascade.

periodic geometry interacting with the circumferentially periodic flow distortions of practical installations should not be lost. Thus, although the aerodynamic response of individual blades and local coupling is of interest, in a larger sense the propeller as a complete geometry must be addressed to characterize the response appropriately.

For turbulence ingestion, the summation of blade lift to form thrust is difficult to calculate because the dynamics governing the interaction of the turbulence with the complex geometry of the propeller make modeling of blade response coupling difficult. However, as a simplifying assumption, the effects can be approximated as a summation gain applied to the blade lift as

$$\Phi_T(\omega) = \lim_{T\to\infty} \frac{2\pi}{T} \left\{ \left[\sum_{i=1}^{B} L_i(\omega)\eta(\bar{\gamma}) \right] \left[\sum_{j=1}^{B} L_j(\omega)\eta(\bar{\gamma}) \right] \right\}$$

$$\equiv |\beta^0(\omega)|^2(\eta(\bar{\gamma}))^2\Phi_L(\omega) \tag{11}$$

where $\eta(\bar{\gamma})$ is a direction cosine to account for average blade pitch and $\beta^0(\omega)$ is the blade summation gain. The blade summation gain $\beta^0(\omega)$ is a dimensionless function that describes nonlinear, blade-to-blade coupling of lift. The superscripted zero denotes that the summation is associated with the coherent thrust. The magnitude of the blade summation gain and extent of thrust production is dependent on the radial distribution of turbulence and blade-to-blade correlation of the lift. The correlation of blade lift is dependent on many factors including radial and circumferential correlation lengths, blade number, blade spacing, and other turbulence quantities. Therefore, although many researchers have addressed an analytic solution for the case of isotropic turbulence, including Sevik,[1] Homicz and George,[15] Mani,[16] and Martinez,[3–5] absolute computation of $\beta_0(\omega)$ is difficult for real flows.

In application to data, the axial blade summation gain is approximated using the sum of a ring of point pressure measurements as addressed in the following section, for now it is assumed known. Thus, the thrust can be obtained from the blade lift and blade summation gain. If the propeller diameter is small and the acoustic range is large relative to the acoustic wavelength, the propeller can be considered a compact acoustic source. Therefore, the acoustic radiation is dominated by a dipole whose source strength depends on the thrust as

$$\Phi_P(\boldsymbol{r}, \omega) = |G_{PT}(\boldsymbol{r}, \omega)|^2\Phi_T(\omega) \tag{12}$$

The notation, $G_{PT}(\boldsymbol{r}, \omega)$, denotes Green's function between far-field pressure and thrust. When Eq. (11) is substituted into Eq. (12), the acoustic radiation is

$$\Phi_P(\boldsymbol{r}, \omega) = |G_{PT}(\boldsymbol{r}, \omega)|^2|\beta^0(\omega)|^2(\eta(\bar{\gamma}))^2\Phi_L(\omega) \tag{13}$$

Furthermore, by the use of Eqs. (7) and (13), the acoustic radiation of the propeller due to thrust can be estimated based only on the turbulence spectrum measured at a single point and the blade summation gain. Ideally, the turbulence measurement should be made in the rotating reference frame to identify modes that are steady in the stationary frame and unsteady in the rotating frame. However, the use of a stationary measurement and an empirically determined summation gain will predict the presence of the broadband and narrowband contributions to thrust associated with these modes although the magnitudes will be understated.

Establishing Blade Summation Gain from Point Pressure Measurement

As in Eq. (11), the blade summation gain is a statement of how the individual blade aerodynamic response will sum to produce the thrust. Complete empirical establishment of the summation gain requires instantaneous knowledge of the pressure everywhere on each blade. However, because this is impractical, the summation gain is approximated by assuming the blade lift is well correlated to the point pressure at 70% of the blade span. Under this assumption, coherent processing of the pressure on each blade gives a time-accurate measure of thrust production. The summation gain of the blade lift, desired for use in Eq. (11), is then approximated by the summation gain of point pressure measurements made along a ring in the propeller plane as shown in Fig. 3a.

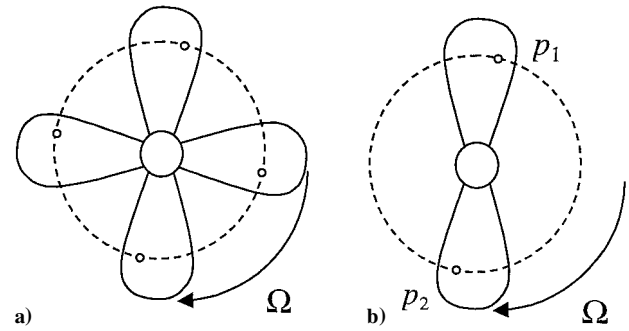

Fig. 3 Example instrumentation of a) four-blade and b) two-blade propellers for empirical estimation of blade summation gain due to turbulence ingestion.

The concept can be understood by considering the simple geometry of the two-blade propeller instrumented with one sensor on each blade, as shown in Fig. 3b. When each blade aerodynamic response is assumed to be statistically distinguishable only by phase due to circumferential location, then the mean-square pressure jump at the same location on different blades will be equivalent. When subscripts 1 and 2 are used to denote blade number, this equivalence can be written as

$$\overline{\langle p^2\rangle} \approx \overline{\langle p_1^2\rangle} \approx \overline{\langle p_2^2\rangle} \tag{14}$$

When the mean square of the sum of the two signals is taken, the value is

$$\overline{\langle p_\Sigma^{0^2}\rangle} = \overline{\langle (p_1+p_2)(p_1+p_2)\rangle} = \overline{\langle p_1^2\rangle} + 2\overline{\langle p_1 p_2\rangle} + \overline{\langle p_2^2\rangle} \tag{15}$$

When Eq. (14) is applied to the right-hand side of Eq. (15), the ratio of the summed pressure to the single point pressure, called the array gain, is

$$\frac{\overline{\langle p_\Sigma^{0^2}\rangle}}{\overline{\langle p^2\rangle}} \approx \left[2 + 2\frac{\overline{\langle p_1 p_2\rangle}}{\overline{\langle p^2\rangle}} \right] = [2 + 2R_{12}(t)] \tag{16}$$

In general, for a propeller with B blades, Eq. (16) becomes

$$\overline{\langle p_\Sigma^{0^2}\rangle} \approx B\overline{\langle p^2\rangle} + 2B\overline{\langle p_i p_j\rangle}|_{|i-j|=1} + 2B\overline{\langle p_i p_j\rangle}|_{|i-j|=2} + \cdots + 2B\overline{\langle p_i p_j\rangle}|_{|i-j|=\mathrm{int}[B/2]-\xi} + B\xi\overline{\langle p_i p_j\rangle}|_{|i-j|=B/2} \tag{17}$$

where ξ is 1 for even B and 0 for odd B. As in Eq. (16), the array gain can be stated in terms of the pressure cross-correlation coefficient on the individual blades as

$$\frac{\overline{\langle p_\Sigma^{0^2}\rangle}}{\overline{\langle p^2\rangle}} \approx B + 2BR_{ij}(t)|_{|i-j|=1} + 2BR_{ij}(t)|_{|i-j|=2} + \cdots + 2BR_{ij}(t)|_{|i-j|=\mathrm{int}[B/2]-\xi} + B\xi R_{ij}(t)|_{|i-j|=B/2} \tag{18}$$

Equations (17) and (18) are arranged, in order of nearest-neighbor correlation, second-nearest-neighbor correlation, and then increasing blade spacing to farthest-neighbor correlation.

To ease interpretation, this expression can be written as

$$\frac{\overline{\langle p_\Sigma^{0^2}\rangle}}{\overline{\langle p^2\rangle}} \approx \left[B + (B^2 - B)\frac{\overline{\langle p_i p_j\rangle}}{\overline{\langle p^2\rangle}} \right] = \left[B + (B^2 - B)R_{ij}(t) \right] \quad \text{for } i \neq j \tag{19}$$

assuming blade-to-blade correlation $[R_{ij}(t), i \neq j]$ is constant for all blade pairs. This assumption does not hold for propellers with many blades ($B \geq 4$) because the variation in blade spacing between

nearest and farthest neighbors becomes significant. However, because the array gain on the left-hand side of Eq. (19) is a measured quantity, the assumption impacts only how the gain is interpreted. Blind use of Eq. (19) for a propeller with many blades to determine $R_{ij}(t)$ from the array gain gives a value that represents a spatial average over the entire propeller.

The utility of the time-domain definition in Eq. (19) is limited to large-scale, spanwise-coherent distortions like those produced by stators or inlet guide vanes. However, for the case of turbulence ingestion, an analogous form of Eq. (18) can be defined as

$$\frac{\Phi_\Sigma^0(\omega)}{\Phi_p(\omega)} \approx B + 2B\gamma_{ij}(\omega)|_{|i-j|=1} + 2B\gamma_{ij}(\omega)|_{|i-j|=2} + \cdots + 2B\gamma_{ij}(\omega)|_{|i-j|=\mathrm{int}[B/2]-\xi} + B\xi\gamma_{ij}(\omega)|_{|i-j|=B/2} \tag{20}$$

As before, assuming blade-to-blade coherence is constant for all blade pairs gives

$$\frac{\Phi_\Sigma^0(\omega)}{\Phi_p(\omega)} \approx \left[B + (B^2 - B)\gamma_{ij}(\omega)\right] \tag{21}$$

Equation (21) is not the exact Fourier equivalent of Eq. (19) because the coherence is not the Fourier equivalent of the cross-correlation coefficient. Thus, application of Eq. (21) in the spectral domain might give misleading results for the propeller in any realizable flow. A particular example would be that case of a circumferentially periodic flow with mode number one off of the blade number. In this case, the coherence between the individual blade responses would be near unity because they would be identical except for a constant phase relationship and Eq. (21) would indicate a large summation gain. However, the measured blade summation gain would be very low, as this mode will produce blade responses that do not coherently sum to produce thrust.

The blade summation gain is approximated by the array gain of the point pressures as

$$|\beta^0(\omega)|^2 \approx \frac{\Phi_\Sigma^0(\omega)}{\Phi_p(\omega)} \tag{22}$$

for application of the earlier two sections to experimental data. Therefore, the blade summation gain responsible for thrust production, as defined, is dependent on the blade-to-blade coherence of the near-field pressure. For the case of incoherent blade aerodynamic response produced by small-scale turbulence, $\gamma_{ij} \approx 0$, the blade summation gain is predicted to be the blade number B, which denotes individual contribution of the blades to unsteady thrust. However, if the turbulence is large, $\gamma_{ij} \neq 0$, the summation gain will be greater than the blade number, which indicates blade-to-blade coupling of the lift to enhance thrust production. In the limit of $\gamma_{ij} \to 1$, the blade summation gain will approach B^2 corresponding to complete constructive summation of mean-square blade lift to produce thrust. Therefore, the blade summation gain becomes a measure of thrust production and radiation efficiency for each of the flow modes.

To this point in the analysis, the superscripted zero on the blade summation gain has been included to indicate axial force but has not differentiated any other notation. In the case of unsteady thrust, the circumferential modes corresponding to multiples of the blade passage frequency produced large axial summation gains. However, the modes one shaft rate from the blade passage frequency, that is, $\omega = (mB \pm 1)\Omega$, are responsible for propeller side forces and give zero axial summation gain. Therefore, a second definition for the blade summation gain is appropriate for estimation of the unsteady side forces produced by the propeller. The transverse summation gain is defined as

$$|\beta^1(\omega)|^2 \approx \frac{\Phi_\Sigma^1(\omega)}{\Phi_p(\omega)} \tag{23}$$

where the numerator of Eq. (23) is the spectral equivalent of

$$\overline{\langle p_\Sigma^{1^2} \rangle} = \left\langle \overline{\left[\sum_{j=1}^{B} p_j e^{i(\theta_j + \Omega t)} \right]^2} \right\rangle \tag{24}$$

Equations (15) and (24) are special cases of the general spatial filter applied to the ring array of sensors on the propeller blades obtained by replacing the exponential in Eq. (24) with $e^{in(\theta_j + \Omega t)}$. The real and imaginary components of Eq. (24) correlate to two orthonormal force components that, when the blade indices θ_j are chosen correctly, correspond to the horizontal and vertical components of the force. When this definition and the appropriate direction cosine in Eqs. (11) and (13) are used, both the side forces and the resulting radiation can be estimated.

Empirical Characterization of Far-Field Response

In addition to completion of the direct solution of the acoustic problem, the blade summation gain can be used to determine radial integral scale and the transfer functions relating pressure to lift and thrust to sound. In Eq. (13), the far-field pressure was approximated using the blade summation gain and the blade lift. Substitution of Eq. (9) into Eq. (13) gives

$$\Phi_P(\boldsymbol{r}, \omega) = 2\Lambda_3 L_3 |G_{PT}(\boldsymbol{r}, \omega)|^2 |H_{lp}(x_1)|^2 |\beta^0(\omega)|^2 \times (\eta(\bar{\gamma}))^2 \Phi_{\Delta p}(x_1, \omega) \tag{25}$$

When the point pressure response is assumed to typify the total blade aerodynamic response, the summed pressure can be substituted:

$$\Phi_P(\boldsymbol{r}, \omega) = 2\Lambda_3 L_3 |G_{PT}(\boldsymbol{r}, \omega)|^2 |H_{lp}(x_1)|^2 (\eta(\bar{\gamma}))^2 \Phi_\Sigma^0 \times (x_1, x_3 = 0.7L_3, \omega) \tag{26}$$

Thus, the acoustic radiation is directly related to the summed point pressures.

Furthermore, the expected cross spectrum between the far-field pressure and the summed pressure can be stated in terms of the summed pressure spectrum. As before, integration along the span gives a single-frequency component of the blade lift as

$$L(\omega) = \pi\rho c U L_3 \int_{-\infty}^{\infty}\int_{-\infty}^{\infty} u_2(k_1, k_3, \omega) S_{2D}\left(\frac{1}{2}k_1 c, \frac{1}{2}k_3 c\right) \times \left(\frac{\sin \frac{1}{2}k_3 L_3}{\frac{1}{2}k_3 L_3}\right) \mathrm{d}k_1\, \mathrm{d}k_3 \tag{27}$$

The radiated acoustic Fourier component at a point in the far field is

$$P(\boldsymbol{r}, \omega) = G_{PT}(\boldsymbol{r}, \omega) T(\omega) = G_{PT}(\boldsymbol{r}, \omega) |\beta^0(\omega)| \eta(\bar{\gamma}) L(\omega) \tag{28}$$

and substituting, one obtains

$$P(\boldsymbol{r}, \omega) = \pi\rho(cL_3) U G_{PT}(\boldsymbol{r}, \omega) |\beta^0(\omega)| \eta(\bar{\gamma}) \int_{-\infty}^{\infty}\int_{-\infty}^{\infty} u_2(k_1, k_3, \omega) S_{2D}\left(\frac{1}{2}k_1 c, \frac{1}{2}k_3 c\right) \times \left(\frac{\sin \frac{1}{2}k_3 L_3}{\frac{1}{2}k_3 L_3}\right) \mathrm{d}k_1\, \mathrm{d}k_3 \tag{29}$$

Therefore, the cross spectrum of the radiated pressure with the summed pressure can be written as

$$\Phi_{P\Sigma}(\boldsymbol{r}, \omega) = \pi\rho(cL_3) U G_{PT}(\boldsymbol{r}, \omega) |\beta^0(\omega)|^2 [\eta(\bar{\gamma})]^2 \times \Delta p(x_1, x_3 = 0.7L_3, k_1, k_3, \omega) \int_{-\infty}^{\infty}\int_{-\infty}^{\infty} u_2(k_1, k_3, \omega) \times S_{2D}\left(\frac{1}{2}k_1 c, \frac{1}{2}k_3 c\right)\left(\frac{\sin \frac{1}{2}k_3 L_3}{\frac{1}{2}k_3 L_3}\right) \mathrm{d}k_1\, \mathrm{d}k_3 \tag{30}$$

When the turbulence is assumed to be homogeneous, the pressure in Eq. (30) can be expressed using Eq. (2) as

$$\Phi_{P\Sigma}(\boldsymbol{r}, \omega) = \rho^2 U^2 \left(\frac{c/2 - x_1}{c/2 + x_1}\right) L_3 G_{PT}(\boldsymbol{r}, \omega) |H_{lp}(x_1)||\beta^0(\omega)|^2 \times (\eta(\bar{\gamma}))^2 \int_{-\infty}^{\infty}\int_{-\infty}^{\infty} \Phi_u(k_1, k_3, \omega) \left| S_{2D}\left(\frac{1}{2}k_1 c, \frac{1}{2}k_3 c\right)\right|^2 \times \left(\frac{\sin \frac{1}{2}k_3 L_3}{\frac{1}{2}k_3 L_3}\right) \mathrm{d}k_1\, \mathrm{d}k_3 \tag{31}$$

When the earlier assumptions of a separable turbulence model, frozen convection, and small integral length scale relative to the blade span are followed, the cross spectrum can be written as

$$\Phi_{P\Sigma}(\boldsymbol{r}, \omega) = \frac{L_3}{\pi} \Lambda_3 G_{PT}(\boldsymbol{r}, \omega) |H_{lp}(x_1)||\beta^0(\omega)|^2 (\eta(\bar{\gamma}))^2 \times \int_{-\infty}^{\infty} \frac{\sin \frac{1}{2}k_3 L_3}{\frac{1}{2}k_3 L_3} \mathrm{d}k_3 \times \left[4\rho^2 U^2 \left(\frac{c/2 - x_1}{c/2 + x_1}\right) \Phi_u(\omega) \left| Se\left(\frac{\omega e}{2U_\infty}\right)\right|^2 \right] \tag{32}$$

Finally, when the integral is evaluated and the pressure spectrum is substituted for the bracketed term in Eq. (32), the result is

$$\Phi_{P\Sigma}(\boldsymbol{r}, \omega) = 2\Lambda_3 G_{PT}(\boldsymbol{r}, \omega) |H_{lp}(x_1)||\beta^0(\omega)|^2 (\eta(\bar{\gamma}))^2 \Phi_{\Delta p}(x_1, \omega) \approx 2\Lambda_3 G_{PT}(\boldsymbol{r}, \omega) |H_{lp}(x_1)| (\eta(\bar{\gamma}))^2 \Phi^0_{\Sigma}(x_1, x_3 = 0.7L_3, \omega) \tag{33}$$

When these definitions are used, estimates of the coherence and frequency response functions between the near and far pressure fields are given as

$$\gamma^2_{P\Sigma}(\omega) = \frac{|\Phi_{P\Sigma}(\boldsymbol{r}, \omega)|^2}{\Phi_P(\boldsymbol{r}, \omega)\Phi^0_{\Sigma}(\omega)} = \frac{2\Lambda_3}{L_3} \tag{34}$$

$$\frac{1}{|H_{P\Sigma}(\boldsymbol{r}, \omega)|} = \frac{\Phi_P(\boldsymbol{r}, \omega)}{|\Phi_{P\Sigma}(\boldsymbol{r}, \omega)|} = L_3 |H_{lp}(x_1)||G_{PT}(\boldsymbol{r}, \omega)| \tag{35}$$

Equation (34) relates the radial integral length scale of the turbulence to the blade span using the coherence between the near and far pressure fields. The relation between the acoustic radiation of the propeller and a circumferentially summed measure might be expected to treat the circumferential modes only. However, the radial and circumferential modes have dependent behavior due to propeller geometry. That is, the turbulence modes with large circumferential scales of low-frequency excite modes near the blade passage frequency producing transference of flow energy from low to high frequency. The small-scale radial modes produce spanwise coherent lift directly converting flow energy into acoustic radiation. The cross-correlation methods, therefore, identify the thrust production due to this latter direct transference of energy. The remaining portion identified by the blade summation gain represents the former portion that is difficult to treat analytically.

Equation (35) uses measurements of the pressure near field and acoustic far field at a minimal number of locations $(B + 1)$ to estimate the two transfer functions. If a simple, free running rotor well described by the dipole model is considered, the cross correlation of near-field and far-field pressures gives a measure of the transfer function between point pressure and section lift. Alternatively, for a more complicated geometry such as a turbojet engine, the dipole model will not hold. In this situation, if the distribution of pressure can be described by some numerical or analytical method, then the cross correlation exposes Green's function governing acoustic radiation. Additionally in such configurations, a summation measurement from each stage establishes the individual stage response when cross correlated with the far field. Therefore, the relationship of the near-field source to the far field is established without modeling the complex geometry or specifically defining the incoming flow.

Discussion

Flowfields composed primarily of large-scale, mean-flow distortions with circumferentially periodic patterns are used in Ref. 17 as a validation tool to demonstrate the use of the blade summation' technique. In these cases, by the varying of the rotational speed of the propeller, the individual blade aerodynamic response can be mapped over a range of frequency giving an empirical measure of the relation between velocity and pressure. The unsteady thrust and acoustic radiation predicted from the summation gain will be compared to measurement of the acoustic radiation. To extend the results to the general case, the methods will then be applied to the propeller ingesting grid-generated, small-scale turbulence. Here, the individual blade aerodynamic response will be interpreted using the relationships obtained in the circumferentially periodic cases and compared to the developments of Eqs. (1) and (2). Again, the total response will be predicted using the empirical summation gain and compared to the measured acoustic radiation.

Conclusions

The analysis treats the complete aerodynamic and aeroacoustic problem for the free rotor ingesting turbulence. However, the results are not limited to this simple case. The incorporation of empirical information to complete the analysis enables direct measurement of the relationship between near-field source and far-field radiation for more complex configurations. The analysis differs from the analytical treatment of other researchers by addressing the propeller problem in a way that has practical significance to empirical data. The empirical data are introduced at the point in the analysis where it is most difficult to proceed analytically but is empirically straightforward due to use of the propellers' own geometry. The analytic and empirical results combine to quantify the production of radiated noise for identification and removal of specific noise sources. Thus, issues due to complex geometry and unknown inflow conditions, which complicate the analytic establishment of these functions, are avoided by use of the empirical definition.

Acknowledgments

This research was performed at the Hessert Center for Aerospace Research, Department of Aerospace and Mechanical Engineering, University of Notre Dame, for the U.S. Navy, Office of Naval Research, Arlington, Virginia, under Contracts N00014-95-1-0488 and N00014-97-0489 and Subcontract N00167-402.15-UND with Cambridge Acoustical Associates, Inc. The authors would like to thank the Program Manager, Lawrence P. Purtell.

References

[1] Sevik, M., "Sound Radiation from a Subsonic Rotor Subjected to Turbulence," NASA SP 304, 1971, pp. 493–511.

[2] Blake, W. K., "Mechanics of Flow-Induced Sound and Vibration," *Applied Mathematics and Mechanics*, Vols. 17-I and 17-II, Academic Press, New York, 1986, pp. 735–752.

[3] Martinez, R., "Broadband Sources of Structure-Borne Noise for Propulsors in 'Haystacked' Turbulence," *Computers and Structures*, Vol. 65, No. 30, 1995, pp. 475–490.

[4] Martinez, R., "Asymptotic Theory of Broadband Rotor Thrust, Part 1: Manipulations of Flow Probabilities for a High Number of Blades," *Journal of Applied Mechanics*, Vol. 63, March 1996, pp. 136–142.

[5] Martinez, R., "Asymptotic Theory of Broadband Rotor Thrust, Part 2: Analysis of the Right Frequency Shift of the Maximum Response," *Journal of Applied Mechanics*, Vol. 63, March 1996, pp. 143–148.

[6] Grace, S. M., Atassi, H. M., and Blake, W. K., "Inverse Aeroacoustic Problem for a Streamlined Body, Part 1: Basic Formulation," *AIAA Journal*, Vol. 34, No. 11, 1996, pp. 2233–2240.

[7] Grace, S. M., Atassi, H. M., and Blake, W. K., "Inverse Aeroacoustic Problem for a Streamlined Body, Part 2: Numerical Accuracy," *AIAA Journal*, Vol. 34, No. 11, 1996, pp. 2241–2246.

[8] Sears, W. R., "Some Aspects of Non-Stationary Airfoil Theory and Its Practical Application," *Journal of the Aeronautical Sciences*, Vol. 8, No. 3, 1941, pp. 104–108.

[9] Patrick-Grace, S. M., and Atassi, H. M., "Inverse Aeroacoustic Problem for a Rectangular Wing Interacting with a Gust," AIAA Paper 96-1790, 1996.

[10]Filotas, L. T., "Theory of Airfoil Response in a Gusty Atmosphere Part I—Aerodynamic Transfer Function," Univ. of Toronto Inst. for Aerospace Studies, UTIAS Rept. 139, Air Force Office of Scientific Research, AFOSR 69-2150TR, Oct. 1969.

[11]Filotas, L. T., "Theory of Airfoil Response in a Gusty Atmosphere Part II—Response to Discrete Gusts or Continuous Turbulence," Univ. of Toronto Inst. for Aerospace Studies, UTIAS Rept. 141, Air Force Office of Scientific Research, AFOSR 69-3089TR, Nov. 1969.

[12]Amiet, R. K., "Compressibility Effects in Unsteady Thin Airfoil Theory," *AIAA Journal*, Vol. 12, No. 2, 1974, pp. 252–255.

[13]Reissner, E., "Effect of Finite Span on the Air Load Distribution for Oscillating Wings, I-Aerodynamic Theory of Oscillating Wings of Finite Span," NACA TN 1196, 1947.

[14]Graham, J. M. R., "Lifting Surface Theory for the Problem of an Arbitrarily Yawed Sinusoidal Gust Incident on a Thin Aerofoil in Incompressible Flow," *Aeronautics Quarterly*, Vol. 21, No. 2, 1969, pp. 182–198.

[15]Homicz, G. F., and George, A. R., "Broadband and Discrete Frequency Radiation from Subsonic Rotors," *Journal of Sound and Vibration*, Vol. 36, No. 2, 1974, pp. 151–177.

[16]Mani, R., "Noise Due to Interaction of Inlet Turbulence with Isolated Stators and Rotors," *Journal of Sound and Vibration*, Vol. 17, No. 2, 1971, pp. 251–260.

[17]Minniti, R. J., Blake, W. K., and Mueller, T. J., "Inferring Propeller Inflow and Radiation from Near-Field Response, Part 2: Empirical Application," *AIAA Journal*, Vol. 39, No. 6, 2001, pp. 1037–1046.

P. J. Morris
Associate Editor